X-Ray Laser Studies at LLE

B. YAAKOBI, D. SHVARTS, T. BOEHLY, P. AUDEBERT, R. EPSTEIN, B. BOSWELL, MARTIN C. RICHARDSON, SENIOR MEMBER, IEEE, AND J. M. SOURES

Abstract—**New target geometries for collisional excitation X-ray laser experiments (in nickel) were proposed, analyzed, and experimentally studied on the GDL laser. Experiments using a short line focus lens with new target geometries showed general agreement with predictions. The new geometries are designed to yield a higher gain and reduced refraction due to 1) a higher plasma density, 2) a wider lateral density profile, and 3) a concave lateral density profile. These new geometries were a) two parallel exploding (thin) foils, irradiated from one side only, b) two ablating (thick) foils, one of which is irradiated on its inner face, and c) an exploding foil in front of an ablating foil, irradiated by a single laser beam incident on the thin foil. New experiments with a long line focus are in progress. The intensity ratio of Ne-like and F-like Ni lines is used to deduce the temperature, and these results together with the absolute intensity yields the density profile. The results show improvement achieved with the new target geometries: the density is higher (leading to a higher gain), and the concave density profile results in collimation rather than divergence of the X-ray laser beam. Theoretical developments included development of a ray-tracing code for an amplifying medium of varying (e.g., collimating) lateral density profile (results using this code are shown for convex as well as concave lateral density profiles) and prediction of high gain on new type transitions in neonlike ions, involving the excitation of an inner (2 s) electron.**

I. Introduction

RECENT X-ray laser experiments [1]–[3] used thin, exploding targets to avoid the steep density gradient characteristic of plasma expansion from thick targets. The thin target explodes and generates a roughly cylindrical plasma having a flat electron density profile of about 3–5 $\times 10^{20}$ cm^{-3}, and a flat temperature profile. The lateral scale-length is of the order of 100–150 μm and the refraction effect is reduced since rays can now propagate 1–2 cm in such a profile before being deflected out of the lasing region.

The exploding foil geometry suffers two drawbacks: first, in order to achieve a symmetrically expanding plasma with a long scale length, the laser must burn through the foil before the peak of the laser pulse. Consequently, the electron density at the time of lasing is only about 4 $\times 10^{20}$ cm^{-3}. This is lower than the density for the maximum gain coefficient by at least a factor of two. Secondly, the refraction effect which was reduced by employing the exploding foil geometry still limits the length of the plasma column to 1–3 cm because the density profile tapers away from the axis. In the new geometries described here, an attempt is made to overcome these limitations. These new geometries, in addition to increasing the density, may either result in wider lasing channels or concave lateral density profiles, both of which reduce refraction losses.

We chose nickel because, for the density range attained in these geometries (in the mid-10^{20} cm^{-3}), it yields a gain coefficient which is close to optimal [4]. Also, nickel requires only modest plasma temperatures (500 to 700 eV) as compared with a higher-Z target. This temperature is compatible with the laser intensity available for the present experiments. Choosing nickel (rather than selenium) leads to longer-wavelength lasing lines, in the range 215 to 300 Å, as compared with 180 to 210 Å for selenium. Since the optimal plasma density (even for nickel) is higher than that occurring in a simple exploding-foil experiment, we have concentrated on new target geometries that can increase the plasma density and lead to a higher gain.

II. Description of the New Geometries

A. Two Exploding Foils

The density profile of a single thin exploding nickel foil is shown schematically in Fig. 1(a). After the initial burn-through a nearly symmetrical expansion is obtained. Although a population inversion is achieved early, the lasing X rays suffer severe refraction losses until the plasma has reached large enough lateral dimensions. An arrangement that can improve the lateral dimension of the plasma consists of two parallel foils facing each other [5] (Fig. 1(b)). The optimal distance between the exploding foils was found to be in the range of 150–250 μm, for an irradiance of the order of 10^{13} W/cm^2. For much larger distances the collision between the two plasmas occur when the density has fallen to too low a level for lasing, whereas for much smaller distances the increase in scale length over the single-foil case is not significant.

The arrangement of two exploding foils offers the following advantages: first, when the plasmas expand inwards from the two foils and collide, a concave density profile forms. Later, the profile is flat-topped with a larger width than in the corresponding single-foil case. Additionally, we have found that a pair of thin foils can be

Manuscript received May 3, 1988; revised May 20, 1988. This work was supported by the Naval Research Laboratory under Contract no. N00014-86-C-2281 and by the Laser Fusion Feasibility Project at the Laboratory for Laser Energetics.

B. Yaakobi, T. Boehly, P. Audebert, R. Epstein, B. Boswell, M. C. Richardson, and J. M. Soures are with the Laboratory for Laser Energetics, University of Rochester, 250 East River Road, Rochester, NY 14623.

D. Shvarts was with the Laboratory for Laser Energetics at the University of Rochester; he is now with the Nuclear Research Center—Negev, Beer-Sheva, Israel.

IEEE Log Number 8823173.

0093-3813/88/1000-0505$01.00 © 1988 IEEE

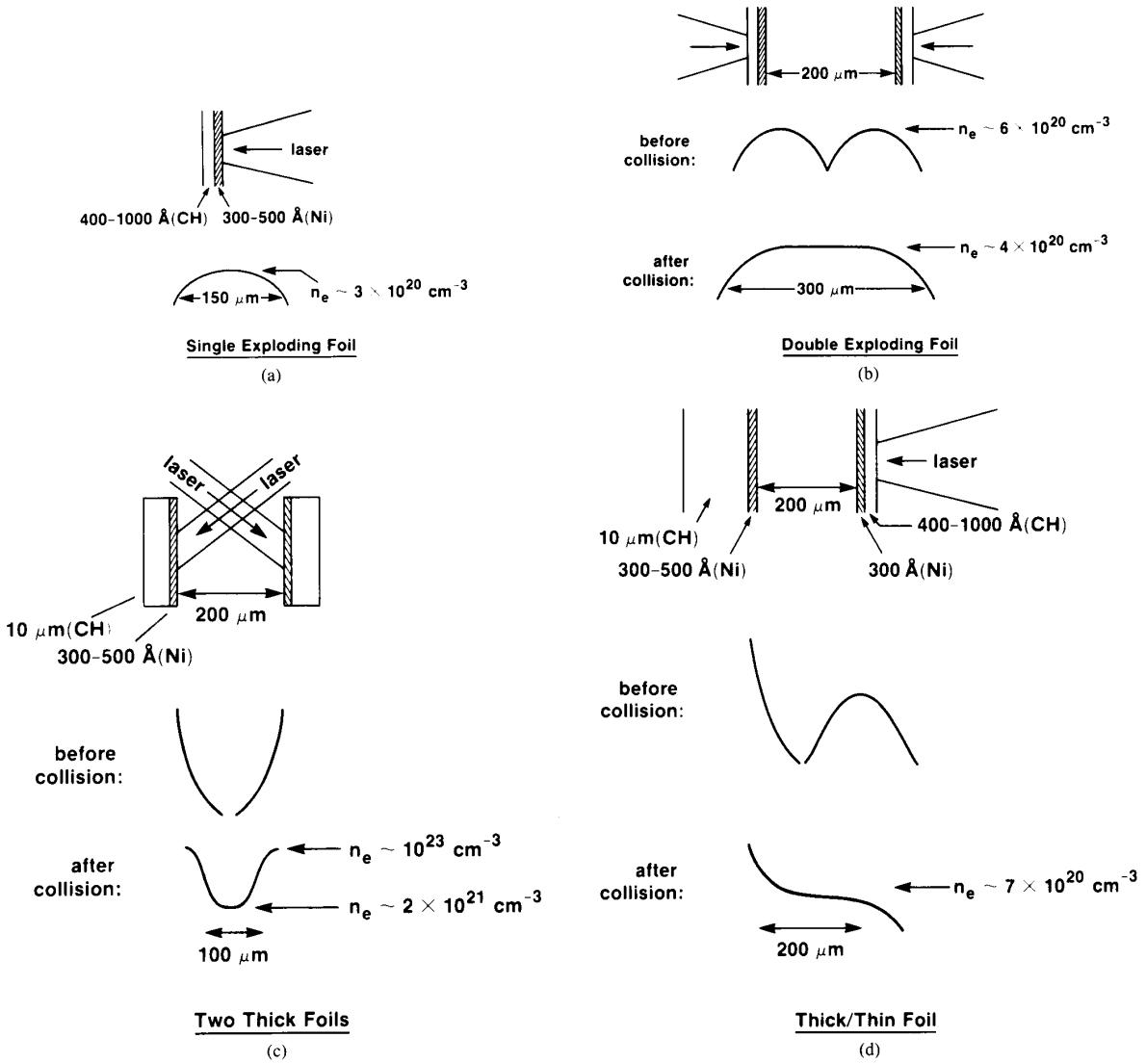

Fig. 1. Schematic spatial density profile of several target configurations discussed in this paper. (a) Single exploding foil. (b) Double exploding foil. (c) Two thick foils. (d) A thick and thin double foil.

irradiated from only one side and still result in density profiles similar to the case where a double foil is irradiated from both sides. In such a design the laser burns through the first foil prior to the peak of the pulse; it is then transmitted through the first-foil plasma and absorbed by the second foil, causing it to explode. A uniform plasma can be formed between the foils even though the interface between the two colliding plasmas will not be on the mid-plane.

B. Two Ablating Slabs

The arrangement of two exploding foils does not result in significantly higher plasma density as compared with the single-foil case. To achieve higher density we have considered a novel geometry, consisting of two slabs (thick foils) irradiated on the inner surfaces (Fig. 1(c)). Since the laser does not burn through these thick foils the resulting density profile falls sharply from either foil towards the mid-plane. A concave profile with a minimum between the slabs is formed. The temperature is uniform between the foils, and it falls sharply near the surfaces of the foils. The ablated material, which is now hydrodynamically confined between the slabs, raises the density throughout the pulse by a factor ten times higher than that attained in exploding-foil geometries. The slab separation can be chosen to yield the optimal density for an extended period of time. Compared to the exploding foils, a potentially higher X-ray laser gain can be achieved with this geometry because of the higher density and because of the collimating effect of a concave density profile. In this ge-

ometry, rays traveling in an off-axis direction will be refracted back into the lasing medium rather than out of it as in the convex density profile of an exploding foil. The higher density may adversely affect lasing if the transverse opacity of transitions to the ground state becomes much higher than 1. This can be particularly severe because the stagnated plasma lacks the velocity gradient which, through the Doppler shift, could mitigate the effect of opacity. The high opacity repopulates the lower level of the lasing transition, leading to a reduction in the population inversion. As a remedy the two foils can be made from thin layers of the lasing material deposited on a thick substrate. The substrate material will provide the hydrodynamic confinement and wave guiding but will not contribute to the populating of the lower laser level via resonant excitations.

C. A Pair of Exploding/Ablating Foils

As in the case of the two thin foils, we have found a simpler version of the two ablative slabs geometry which retains some of its advantages. In this simplified version a thin foil is placed in front of a thick foil and is irradiated by a single laser beam (Fig. 1(d)). The laser irradiates the thin foil, burns through it before the peak of the pulse, and then irradiates the thick foil. The collision between the plasmas of the exploding thin foil and ablating thick foil forms a plateau on the falling density profile of the thick foil. The resulting density is higher than that attained in exploding foil plasmas. The scale length of this plateau is about equal to the original foil separation. The advantage of a high density, inherent in the thick-foil case, is partially retained. However, the advantage associated with a concave density profile is retained now only for rays traveling towards the thick foil.

III. Experimental Results

A. Hydrodynamic Studies with Short Line Focus

We describe a series of experiments aimed at measuring the spatial profile of Ne-like nickel plasmas produced by double-foil targets. The initial experiments utilized a 1.5 mm line focus which was of sufficient length for studying the hydrodynamic behavior of the proposed new geometries. Results of experiments using a 1-cm line-focus, which indicate gain in these targets, are also presented. In all cases the target material was nickel.

The experiments were performed using the glass development laser (GDL) single-beam laser system. The targets were irradiated by 600-ps pulses of 527-nm laser light at intensities of $1\text{–}3 \times 10^{13}$ W/cm^2. With shorter irradiation wavelengths the plasma of an exploding foil becomes underdense earlier in time and absorbs less. However, in the nonexploding geometries shorter wavelength illumination is preferable because of the higher mass ablation rate. A cylindrical corrector lens was fitted onto the f/3 aspheric focusing lens to provide a line focus 1.5 mm long and about 50 μm wide at the best focus position. Since a small width may give rise to a two-dimensional plasma expansion, which would severely degrade the density and temperature profiles, we defocused the beam to yield a width of about 100 μm (at larger widths the irradiance is too small).

The thin foils were 300-Å-thick to 800-Å-thick layers of nickel, supported by Formvar ($C_{11}H_{18}O_5$) substrates 400 Å thick. Such substrates have a very small mass compared with that of the nickel foil and hardly affect the hydrodynamic behavior of the foil. An X-ray crystal spectrometer equipped with a 12-μm entrance slit was used to measure the spatially resolved Ni spectra from these targets in the 7 Å to 14 Å range. The spatial resolution is in the direction perpendicular to the foil plane, which is along the distance between the two foils. These spectra can be used to determine the plasma temperature and density. Additionally, we used a pinhole camera to measure the focal spot characteristics and also to observe the two-dimensional plasma behavior (along the line focus direction as well as that which is normal to that direction). This information is important in evaluating the hydrodynamic performance of the new geometries. The XUV spectra in the 40 eV to 250 eV range were measured using a 1-m grazing incidence grating spectrograph. Finally, time-resolved measurements of the laser light transmitted through the target were made in order to determine the occurrence of timely burn-through which is necessary for the formation of a flat density profile.

Fig. 2 shows a typical X-ray spectrum obtained from a thick (about 100 μm) nickel target irradiated at 1×10^{13} W/cm^2. Lines from the NiXIX to NiXXII states of ionization (Ne-, F-, O-, and N-like ions) are seen. The individual Ne-like and F-like lines can be distinguished while the emission from the other ionization species appear as unresolved transition arrays. The lines labeled in Fig. 2 are some of the various Ne-like and F-like transitions that were identified using a relativistic atomic structure code [6]. We use the relative intensity of the $2p^6$–$2p^5 3s$ and $2p^6$–$2p^5 3d$ resonance transitions in the Ne-like ions and the analogous $2p^5$–$2p^4 3s$ and $2p^5$–$2p^4 3d$ resonance transitions in the F-like ions to estimate the relative fractional population of these species (from which temperature can be inferred).

Fig. 3 shows three line-outs of the spatially resolved X-ray spectrum from a double thin-foil target with a spacing of 270 μm and with a laser irradiance of 1.8×10^{13} W/cm^2. These two foils were spaced far enough apart so that the individual foil expansions can be discerned in the X-ray spectral image. The three intensity-corrected spectra correspond to three positions: near the back foil, between the foils, and near the front foil (each spectrum has been normalized to the maximum of spectrum (c)). Note that the spectra at (a) and (c) show significant amounts of Ne-like line emission whereas in the central region the Ne-like line emission is less pronounced. The ratio of F-like to Ne-like line emission was found to be lower in the central region compared to the ratio near the foils, indicating a lower temperature in that region. In addition,

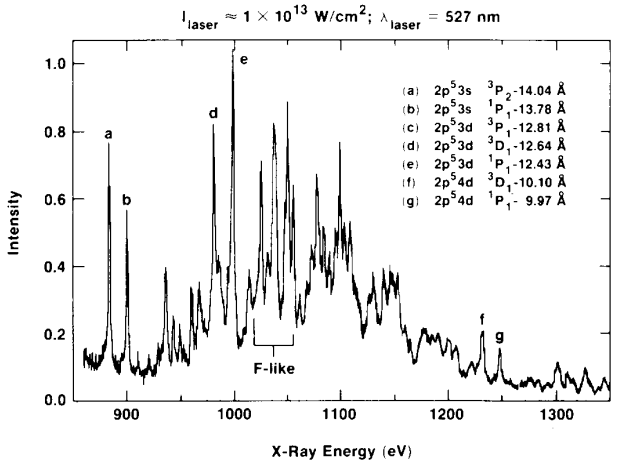

Fig. 2. A sample X-ray spectrum from a massive nickel target. The lines designated by letters a through e are the $n = 3$ to $n = 2$ lines of Ne-like nickel. The lines f and g are due to $n = 4$ to $n = 2$ transitions. The incident laser intensity was 10^{13} W/cm^2.

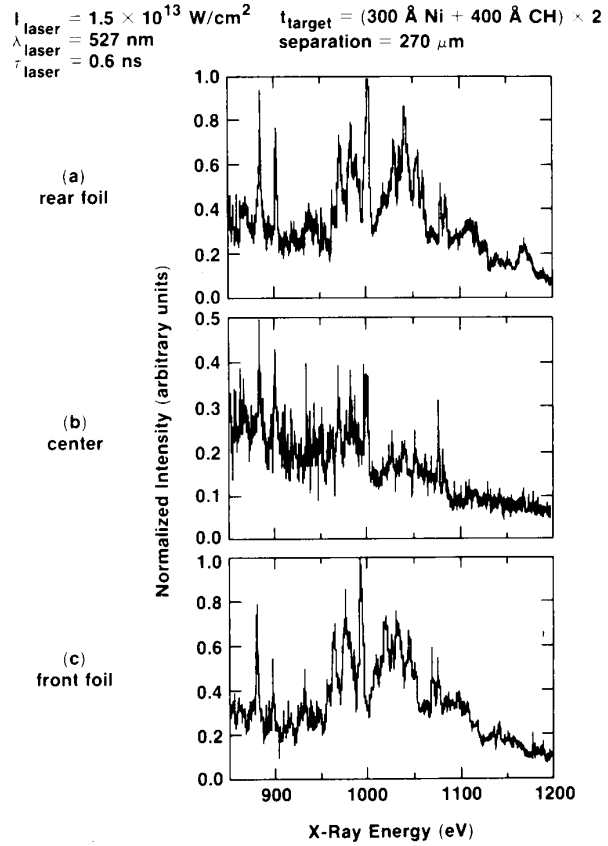

Fig. 3. The X-ray spectra at various positions in a target consisting of two thin (exploding) nickel foils. The spectra are at (a) the rear foil, (b) the central region, and (c) the front foil. The intensity of each spectrum has been normalized to the peak emission in the (c) spectrum. The spectra (especially (a) and (c)) are dominated by neonlike nickel lines.

the overall lower intensity in the center indicates a lower density there.

Fig. 4 summarizes the performance of the new geometries in these experiments. It shows the measured intensity of the Ne-like $2s^2 2p^6$–$2s^2 2p^5 3d$ line (line e in Fig. 2) for the various targets described above. The curves are plotted on the same scale but each target has a different irradiated intensity (the laser energy used at each case is specified; the intensity at each case is proportional to the laser energy). This figure shows the relative performance of the various targets to produce large regions of Ne-like ion populations that can be used as X-ray laser gain media.

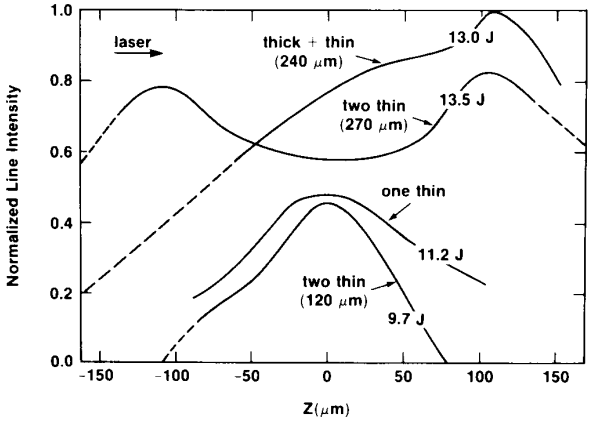

Fig. 4. A comparison of the measured intensity of the Ne-like $2s^2 2p^6$–$2s^2 2p^5 3d$ line (line e in Fig. 2) for the various targets described above. The curves are plotted on the same scale but each target has a different irradiated intensity (the laser energy used at each case is specified; the intensity at each case is proportional to the laser energy). This figure shows the relative performance of the various targets to produce large regions of Ne-like ion populations that can be used as X-ray laser gain media.

sity of the Ne-like $2s^2 2p^6$–$2s^2 2p^5 3d$ line (at 12.4 Å) for the various targets described above. All the curves in this figure have the same scale. The laser energy was different in these experiments, but indications from the simulations indicate that the absorbed energy differences were smaller. Comparison of the two lower curves shows that two foils that are too closely spaced behave essentially like a single foil (the slightly wider profile of the single foil can be attributed to the different laser energy). Three features are particularly notable in Fig. 4: a) the plateau exhibited by the target has one thin and one thick foil, b) the wide and concave profile in the target has two widely spaced thin foils, and c) the higher intensity from both of these targets (as compared with a thin target) is indicative of a higher density.

B. Indication of Gain in Longer Line Focus Experiments

Experiments were performed using a 8-mm line focus and several types of targets. This length of line is marginally adequate for the observation of gain in these targets. In fact, several attempts to observe gain in single exploding foil targets failed to provide even observable intensities for the lines which are expected to lase. However, we were able to observe several of the lines which were expected to lase when irradiating a thin-plus-thick double-foil target (see Fig. 1) that was 8 mm in length. These lines were not observed in any off-axis spectra nor on-axis spectra from targets which were 5-mm in length. This indicates much faster than linear growth of the intensity of these lines with the plasma length. Fig. 5 is a segment of the on-axis XUV spectra from similar double-foil targets which were 8 mm and 5 mm in length. The lines at 296 Å and 301 Å are the $2s^2 2p^5 3p$–$2s^2 2p^5 3s$, $J = 2$ to $J = 1$ transitions and have been observed for single foil experiments at other laboratories [4], [5]. In addition,

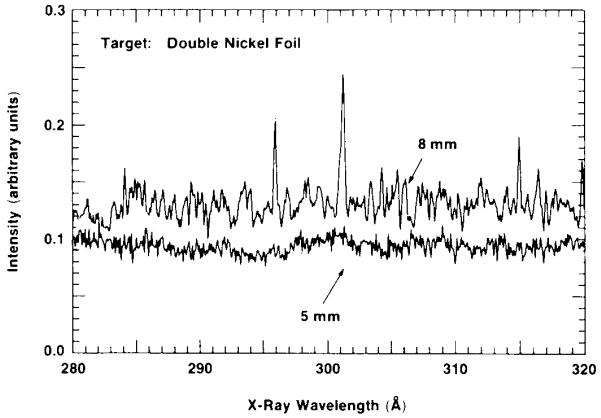

Fig. 5. The XUV spectra from similar double-foil targets which were 8 mm and 5 mm in length. The lines at 296 Å and 301 Å are the $3p(J = 2)$ to $3s(J = 1)$ lines. In addition, the $3p(J = 0)$ to $3s(J = 1)$ line around 215 Å was also observed on this shot.

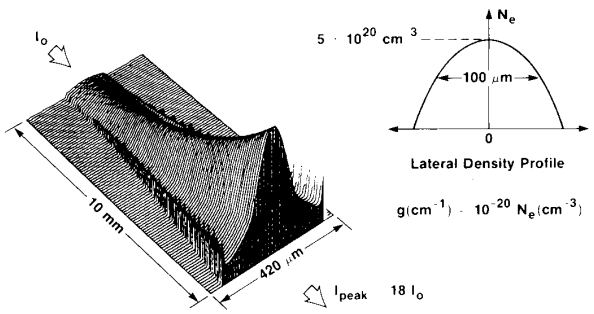

Fig. 6. The calculated X-ray intensity distribution along an amplifier with a convex parabolic density profile. The input beam is a plane wave with a Gaussian intensity distribution (in the lateral coordinate). The density profile and the assumed gain-density relation are also shown.

the $2s^22p^53p$–$2s^22p^53s$, $J = 0$ to $J = 1$ line at around 215 Å was similarly observed for this shot. Although we do not have sufficient line length to perform reliable gain measurements, these results indicate that the double-foil targets outperform the single foil targets. These encouraging results should permit the measurement of gain for various target types in current experiments which use a 20-mm long line focus.

IV. X-Ray Laser Beam Optics

As discussed above, refraction due to electron density gradients plays an important role in determining the effective gain-length product of the X-ray laser. We have developed a geometric-optical model similar to that used by London [7] to examine the effects of refraction on the propagation and amplification of the X-ray beam in both convex and concave lateral density profiles. Two configurations have been examined: the amplified spontaneous emission configuration in which spontaneous emission throughout the plasma is amplified, and the laser-amplifier configuration where an input laser beam enters the medium and is amplified. The main features of behavior are similar in both cases. We will examine the second of the two, i.e., a laser amplifier which has as its input a beam with a Gaussian intensity distribution. Fig. 6 shows the intensity profile of the amplified X-ray radiation for the convex plasma density profile that is shown in the figure. The gain of the amplifier is assumed to be linearly proportional to the plasma density. The dimensions and shape are typical of a single exploding-foil target. In the convex profile the refraction causes a spread in the central peak (amplification alone would have caused a narrowing of this profile). The refraction that causes this broadening reduces the intensity at the center with respect to that which would have occurred in the absence of refraction. Besides the broadening, refraction causes rays to exit the plasma before traveling the entire amplifier length. Some of the rays which exit can be seen in the intensity peaks which occur at the edge of the beam.

Fig. 7 shows the intensity distribution for a concave plasma density profile which is typical of a target consisting of two ablating foils. We also assume that the gain is linearly proportional to the density except for densities greater than 10^{21} cm^{-3} where the gain is set to zero. This assumption simulates the degradation of the population inversion which occurs at higher densities (as well as a result of the falling temperature near the foil surfaces). In the concave profile the behavior is more complex than that shown in Fig. 6. The concave parabolic shape of the density profile serves to contain the rays within the medium, causing them to travel along sinusoidal trajectories. In this calculation we assumed an input beam consisting only of parallel rays. Since the trajectory of a ray is uniquely determined by the incident angle and lateral position of the ray, Fig. 7 represents a unique group of rays. The input rays converge to the axis, then travel outward until they are reflected by the higher density "walls." The peaks along the axis arise from the focusing which occurs at the nodes of the ray trajectories. For the case where the input rays and the spontaneous emission are emitted in all directions, these focal spots would, of course, be smeared along the axis. The ridges in the figure result from the rays which experience the maximum possible gain-length. These rays have turning points at 10^{21} cm^{-3}.

The effect of refraction in the two geometries is summarized in Fig. 8. Here the final gain is calculated with and without refraction, and their ratio η_{ref} is plotted as a function of amplifying medium length. The gain is simply the logarithmic ratio of output to input power. The advantage of the concave geometry is seen to be in limiting the refraction losses for long amplifiers; however, refraction causes losses in both cases.

As the length of the plasma increases the gain reduction ratio approaches a limit. This limit is characteristic of the lateral plasma profiles and applies to both the amplifier and ASE operation. It also scales rather simply with our

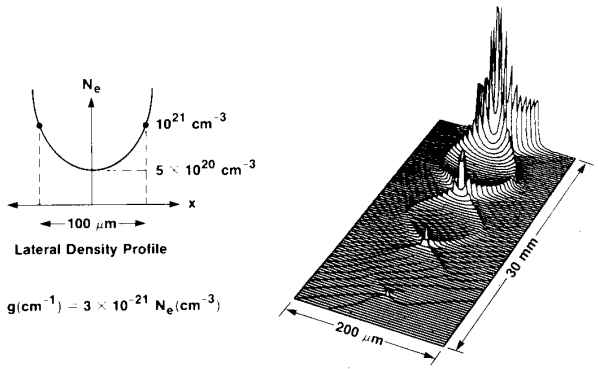

Fig. 7. The calculated X-ray intensity profile along an amplifier with a concave parabolic density profile (in the lateral direction). The input beam has a Gaussian lateral intensity distribution. The gain (proportional to the density) is set to zero for densities greater than 10^{21} cm^{-3}.

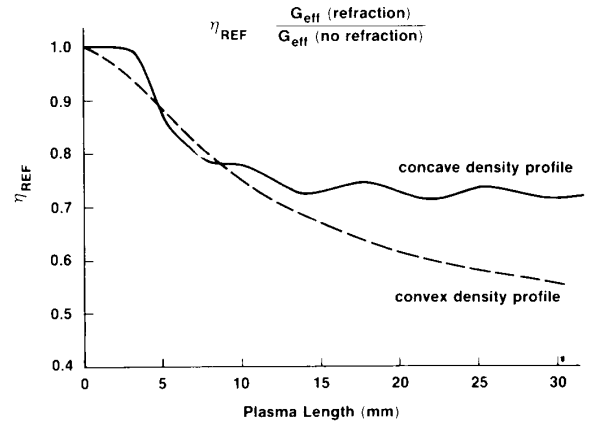

Fig. 8. Degradation in gain due to refraction in the convex and concave geometries. The assumed parameters in these calculations are those in Figs. 6 and 7.

plasma parameters:

$$\eta_\infty = \begin{cases} 1 - \left(\sqrt{\dfrac{N_c}{2N_{\text{axis}}}}\, L_\perp\, g_{\text{axis}} \right)^{-1} & \text{(convex profile)} \\ 1 - \dfrac{1}{2}\left(\dfrac{g_{\text{axis}}}{g_{\max}} \right). & \text{(concave profile)} \end{cases}$$

For the convex case, N_c is the critical electron density for the X-ray wavelength, $L_\perp$ is the FWHM of the profile, and the subscript "axis" refers to the central axis (peak density). The initial term of unity is the ratio corresponding to no effect of refraction. The following term embodies the loss of gain associated with the refraction. The convex loss is inversely proportional to profile width; this is consistent with the results of [7]. In the concave case, g_{axis} is the gain at the density minimum, and $g_{\max}$ is the maximum gain present in the plasma. Here η_∞ does not depend explicitly on the profile width but only on the center and peak gains. Finally, we note that the ideal situation is a flat profile, for which $\eta_\infty = 1$. In the convex case this corresponds to $L_\perp = \infty$, and in the concave case, to $g_{\max} = g_{\text{axis}}$.

In the final analysis the performance of each geometry will be determined by the net gain-length, the refraction losses, and the laser-beam divergence. Since the aspect ratio of each geometry is very large, the path-lengths of all X rays are about equal and the gain-length is then determined by the plasma density. The refraction losses and the output beam divergence depend upon the density profile and somewhat on its magnitude. A detailed analysis of these effects for each geometry is in progress.

V. Gain Calculation for Neon-Like Lines

Gain calculations for a variety of neon-like nickel lines have been carried out using a relativistic, multiconfiguration atomic structure code, coupled to a rate equation package [6]. These calculations are essential in pointing to ways of optimizing gain. The main findings of this analysis can be summarized as follows: a) It is imperative to try and increase the plasma density corresponding to the lasing conditions, from the low 10^{20} to the high 10^{20} cm^{-3} range (this conclusion has been the driving force behind this series of experiments), and b) a new type transition shows promise of being a lasing candidate and should be further explored.

The model used is simplified in certain respects but is sufficient to show the salient features of the inversion mechanisms. A homogeneous, cylindrical plasma is assumed, with equal ion and electron temperatures (750 eV in the example shown here). A rate equation program calculates the distribution of charge states, for the assumed temperature and for a variety of electron densities. For example, the fraction of neon-like nickel for the conditions shown here is around one-third. An important parameter affecting the populations and therefore the gain is the opacity (primarily of the transitions to the ground state). The effect of opacity is determined using the escape factor approximation. The atomic structure code calculates the levels arising from the pertinent configurations and the transition probabilities between them. A detailed calculation of the collisional and radiative transitions between the relevant levels determines the populations and, hence, any possible inversion. This inversion coupled to the line width (determined by the ion temperature) finally yields the gain per unit length.

Fig. 9 shows the results of such calculations for three lines. Line A is the line which defied gain observation in the successful neon-like gain experiments [2]. As for other atomic species, the calculated gain for this line is higher than that for other lines (contrary to observation) for a reason which is not fully understood. Line B is one of the two transitions which showed the highest gain [2]. For clarity we show only one of these two lines. Line C is the new transition involving an inner electron excitation ($2s$ to $3d$). The excitation energy for this transition (1127 eV) is only slightly higher than, say, that from the $2p$ to the highest $3d$ level (998 eV). Fig. 9 shows the significant reduction in the gain when opacity is accounted for. Ad-

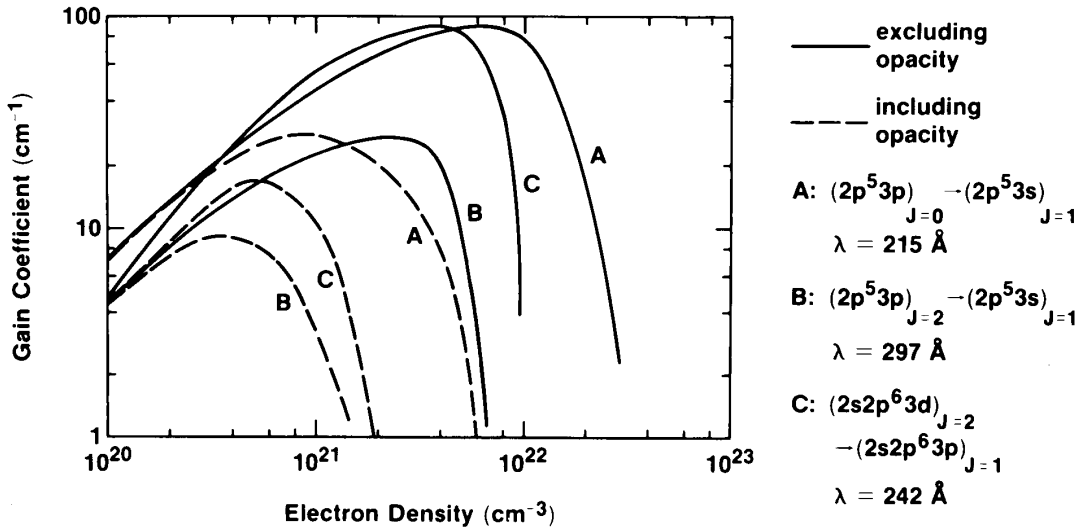

Fig. 9. Model gain calculations for neonlike nickel. A detailed atomic model is coupled to a uniform cylindrical plasma with $T_i = T_e = 750$ eV. A cylindrical uniform plasma of diameter 100 μm was assumed. The line C is a new transition involving the excitation of an inner electron.

ditionally, the gain drop with increasing density occurs at a lower density when opacity is included. Still, it is evident that significant improvement can result from going to higher densities than those prevailing in single exploding-foil experiments. It is also evident that line C (which has not yet been reported to lase) is predicted to show a higher gain than the lasing line B.

References

[1] M. D. Rosen *et al.*, "Exploding-foil technique for achieving a soft X-ray laser," *Phys. Rev. Lett.*, vol. 54, pp. 106-109, 1985.

[2] D. L. Matthews *et al.*, "Demonstration of a soft X-ray amplifier," *Phys. Rev. Lett.*, vol. 54, pp. 110-113, 1985.

[3] D. Matthews *et al.*, "X-ray laser research at the Lawrence Livermore National Laboratory Nova laser facility," *J. Opt. Soc. Amer. B*, vol. 4, pp. 575-587, 1987.

[4] U. Feldman, J. F. Seely, and A. K. Bhatia, "Scaling of collisionally pumped 3s-3p lasers in the neon isoelectronic sequence," *J. Appl. Phys.*, vol. 56, pp. 2475-2478, 1984; A. Bar-Shalom, private communication.

[5] M. D. Rosen and P. L. Hagelstein, "Progress in the analysis of selenium X-ray laser targets," Report UCRL-94412, Mar. 1986.

[6] M. Klapisch, J. L. Schwob, B. S. Fraenkel, and J. Oreg, "The 1s-3p Kβ-like X-ray spectrum of highly ionized iron," *J. Opt. Soc. Amer.*, vol. 67, pp. 148-155, 1977; M. Klapisch, "A program for atomic wavefunction computations by the parametric potential method," *Comp. Phys. Comm.*, vol. 2, pp. 239-260, 1971; A. Bar-Shalom, private communication.

[7] R. A. London, "Beam optics of exploding foil plasma X-ray lasers," *Phys. Fluids*, vol. 31, pp. 184-192, 1988.